

Using the Quadratic Logistic Equation To Analyze Intercalation of Lithium Ions in Layer-by-Layer V₂O₅ Films

Fritz Huguenin,[†] Francisco C. Nart,[‡] Ernesto R. Gonzalez,[‡] and Osvaldo N. Oliveira, Jr.*[§]

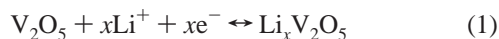
Departamento de Química, Faculdade de Filosofia, Ciências e Letras de Ribeirão Preto, Universidade de São Paulo, 14040-901 Ribeirão Preto (SP), Brazil, Instituto de Química de São Carlos, Universidade de São Paulo, 13560-970 São Carlos (SP), Brazil, and Instituto de Física de São Carlos, Universidade de São Paulo, CP 369 13560-970 São Carlos (SP), Brazil

Received: March 4, 2004; In Final Form: September 15, 2004

The quadratic logistic equation (QLE) is used to determine the number of electrochemical active sites in V₂O₅ films, by fitting the absorbance changes resulting from the intervalence transfer V(IV) → V(V) in chronopotentiometry and cyclic voltammetry experiments. Approximately 20% of the V₂O₅ sites were found to be inactive electrochemically. The absorbance data at 660 nm as a function of the charge injected in layer-by-layer (LBL) films of V₂O₅ alternated with poly(ethylene oxide)/chitosan blend was fitted with the QLE, from which the polaronic transfer between V₂O₅ sites could be investigated. The maximum charge injected was 8 mC cm⁻² for a 15-bilayer LBL film of V₂O₅/blend, with ca. 4.0 × 10⁻⁸ mol cm⁻² of electrochemically active V₂O₅ sites in this film. Departures from the theoretical predictions are interpreted in terms of structural changes in the nanostructured LBL film caused by intercalation of lithium ions. In discussing further applications of the QLE to analyze chemical reactions, it is shown how the number of V(IV) sites is affected by irradiation with a Hg lamp of a 15-bilayer LBL film of V₂O₅/blend.

Introduction

Control at the molecular level is a key factor for developing novel materials with enhanced properties, including those for microbatteries and electrochromic devices. In recent works,^{1,2} it has been shown that the layer-by-layer (LBL) technique,³ which leads to nanostructured films, may be exploited to enhance the charge storage capability of V₂O₅ systems. In the LBL films, V₂O₅ layers were alternated with layers of polyaniline (PANI) or poly(ethylene oxide) (PEO). The interest in V₂O₅ has been considerable because its xerogels may be used as host matrixes for lithium ions in cathodes for secondary lithium batteries and as counter-electrodes in electrochromic devices.^{4,5} The property of interest in these applications is the V₂O₅ xerogel lamellar structure that allows Li⁺ insertion/deinsertion during the injection/expulsion of electrons in the conduction band of the oxide. These processes can be represented by



The optimization of V₂O₅ properties requires understanding the intercalation mechanism of lithium ions, for which a successful model is the so-called small-polaron theory.⁶ The term small polaron, referring to the unpaired electrons in eq 1, is attributed to the strong electron–phonon coupling.⁶ Experimentally, the intercalation of ions can be probed by monitoring light absorption. For example, the polaron jump between vanadium V(IV) and V(V) sites is responsible for a broad band absorption in the near-infrared region, at approximately 850 nm.^{7,8} During

the intercalation of lithium ions, V(IV) sites are formed and the absorbance change (ΔA) increases due to the simultaneous formation of polarons, which yields a higher intervalence transfer V(IV) → V(V) flux. Upon further increasing the charge injected, the intervalence transfer V(IV) → V(V) flux decreases due to an excess of V(IV) sites in comparison with V(V), thus decreasing ΔA . The intercalation process of lithium ions can therefore be understood in terms of the profile of absorbance change as a function of the charge injected.

In this paper we employ the quadratic logistic equation (QLE) to relate the absorbance change to the charge injected in LBL films prepared from V₂O₅ and a blend of poly(ethylene oxide) (PEO) and chitosan. PEO complexes with alkali metal salts are known to possess higher ionic conductivity than other solid-state ionic conductors.⁹ In our first attempts, we found that the adsorption of alternate layers of PEO and V₂O₅ was not efficient, which prompted us to use a blend of PEO and chitosan, thus forming the V₂O₅/blend alternated LBL films. The choice of chitosan, in particular, was based on its ability to complex with metal ions or oxides in solutions.¹⁰ These LBL films were chosen due to their uniformity and reasonable electrochromic properties.² In a previous paper,² we presented results from characterization of LBL films from V₂O₅/blend using UV–vis absorbance and FTIR spectroscopies, from which the structural properties and the interaction among the components could be inferred. Of particular relevance was the complexation between Li⁺ ions and PEO.

The QLE, in both difference and differential forms, is used in mathematical models describing one-variable systems whose temporal evolution is governed by dissipation and feedback or equivalent phenomena.¹¹ For example, the QLE has been used to describe population growth in biological systems and to model physicochemical processes in fuel cells with polymeric electrolytes and the charge transport in thin inorganic and organic

* Corresponding author. E-mail: chu@ifsc.usp.br.

[†] Departamento de Química.

[‡] Instituto de Química.

[§] Instituto de Física.

films.^{12–14} In the context of this paper, the QLE is employed to describe the temporal evolution of the number of polarons ($N_{V(V) \rightarrow V(IV)}$) participating in the intervalence transfer in V_2O_5 films. The intercalation process of lithium ions is considered as a growth step $N_{V(V) \rightarrow V(IV)}$ when $N_{V(V)} \geq N_{V(IV)}$ and as a death step when $N_{V(V)} \leq N_{V(IV)}$. Thus, changes in the rate of $N_{V(IV) \rightarrow V(V)}$ are represented by the change in absorbance, ΔA , as a function of the charge injected. As the charge transferred increases, so does the number of transported electrons and lithium ions. The interactions between these moving charges cause the appearance of dissipative forces, which increase with increasing transported charges, thus contributing to the feedback effect. That is to say, the dissipative forces that oppose the charge transport increase with the amount of charge transported. The feedback effect is also caused by a decrease in the number of sites available for intervalence transfer. Thus, with the increase in the number of electrons and lithium ions intercalated, the intervalence charge-transfer becomes more difficult; i.e., the intervalence transfer process is subjected to dissipation and feedback. This is why the QLE explains the interrelations among the three processes: charge transfer, lithium ions intercalation and absorbance changes. The mathematical expression, which is a direct application of the QLE in its difference form,¹¹ is

$$\Delta A = rq \left(1 - \frac{q}{K} \right) \quad (2)$$

where q is the charge injected, K is associated with the system's ability to sustain the population growth ($N_{V(IV) \rightarrow V(V)}$), representing the maximum value of q , and r is a positive constant. The term $(1 - q/K)$ represents the effects of dissipation and feedback, which increase with q . Though ΔA tends to increase initially with q because more polarons are formed, it decreases at large values of q due to the term $(1 - q/K)$. The similarity between eq 2 and the equation proposed by Austin and Mott for the electrical conductivity in amorphous transition metal oxides provides further support for the use of QLE to interpret ΔA values.^{6,15} In fact, not only the absorbance change but also the conductivity is associated with the polaronic jump $V(IV) \rightarrow V(V)$. The constant r in eq 2 in the small-polaron theory would depend on parameters such as the average hopping distance, the decay rate for the wave function, and the phonon frequency.¹⁵ According to the concepts of dissipation and feedback contained in the QLE, eq 2 shows that ΔA will increase linearly with q only for small values of q . However, for increasing values of charge flows the term $(1 - q/K)$ retards the increase in ΔA , which reaches a maximum and eventually decreases.

Here the QLE is used to fit the absorbance data of V_2O_5 for varying injected charges in LBL films, obtained from chronopotentiometry and cyclic voltammetry experiments. Using the LBL technique is important because it leads to uniform films with precise thickness control, which is essential for the reproducibility of the ΔA data to apply the QLE. Significantly, the amount of electrochemically active sites of V_2O_5 xerogel that may be reduced in chemical reactions could be estimated. Moreover, observation of structural distortions to accommodate the lithium ions could be interpreted and predicted with the QLE.

Experimental Section

V_2O_5 xerogel was synthesized following a sol–gel method described in the literature.¹⁶ Briefly, 0.2 cm³ of vanadyl tri-(isopropoxide), $VC_9H_{21}O_4$ (Gelest), were added to 100 cm³ of pure water. The yellowish liquid obtained was evaporated by heating under vacuum at 70 °C. This procedure was interrupted when the concentration of V_2O_5 reached 0.02 mol L^{−1}. Chitosan

of molecular weight of 9000 g/mol and degree of acetylation equal to 14 was synthesized using the method described in the literature.¹⁷ Poly(ethylene oxide), PEO, was used as received from Aldrich (10000 molecular weight). Layer-by-layer (LBL) films were assembled onto indium–tin oxide (ITO) coated glass purchased from Delta Technologies, with a sheet resistance $\leq 20 \Omega$ and geometrical area of 1 cm². The layers were obtained via ionic attraction of oppositely charged materials, by the alternated immersion for 1 min of the ITO substrate into the polycationic and anionic solutions. The former was either a chitosan solution (1.6 g dm^{−3}) or a blend solution (1.6 g dm^{−3}) of PEO (99%) and chitosan (1%). The polyanionic solution was 0.02 mol L^{−1} V_2O_5 in pure water. The LBL films of V_2O_5 xerogel will therefore be referred to here as V_2O_5 /chitosan and V_2O_5 /blend films. After deposition of each layer, the substrates were rinsed for 30 s in HCl solution (pH = 2) and dried under a nitrogen flow. The films formed had 8, 15, and 60 bilayers and are referred to as 8-, 15-, and 60-bilayer films.

Film growth was monitored by measuring the ultraviolet–visible (UV–vis) absorption spectra of the samples with a Hitachi U-3501 spectrophotometer. The absorbance change showed that the amount of V_2O_5 adsorbed in a V_2O_5 /blend increases almost linearly with the number of bilayers. The thickness of 15-bilayer LBL films measured with a Talystep profilometer was 80 and 45 nm for V_2O_5 /chitosan and V_2O_5 /blend, respectively. The films formed are visually uniform and had root-mean-square roughness of 3 and 5 nm for V_2O_5 /chitosan and V_2O_5 /blend, respectively, as determined from atomic force microscopy (AFM) measurements performed in a SPM Multimode–Nanoscope III from Digital Instruments using the tapping mode. X-ray diffraction of the LBL films was carried out on a Carl Zeiss URD-6 diffractometer using monochromatic Cu K α radiation. The diffractogram (result not shown) indicated that the degree of crystallinity was very small.

For the electrochemical experiments, the counter electrode was a platinum sheet with an area of 10 cm². The quasi-reference electrode was saturated Ag/AgNO₃. An electrolytic solution of 0.5 mol L^{−1} LiClO₄ (Aldrich, 99.99%) in propylene carbonate (PC) (Aldrich, anhydrous 99.7%) was used in all experiments carried out with an Autolab PGSTAT30 potentiostat/galvanostat. Chromogenic analysis was made simultaneously with the electrochemical experiments using a microprocessor-controlled solid-state light source (WPI, Inc.). Plastic fiber optic cables up to 1 mm in diameter were used to deliver red light (660 nm) from the instrument to a PDA1 photodiode amplifier (WPI, Inc.). To obtain the mass of cast $V_2O_5 \cdot 1.6H_2O$ xerogel, a quartz crystal microbalance (EQCM) was used. The substrates were 6 MHz AT-cut quartz crystals coated with Pt with a piezoelectric active area of 0.31 cm². The resonance frequency shift was measured with a HP-5370B Universal Time Counter.

Results and Discussion

To validate the use of the logistic equation (QLE) in explaining changes in ΔA due to the $V(IV) \rightarrow V(V)$ intervalence transfer, it is necessary to know the total number of V_2O_5 sites in the material. This number can be easily obtained in thick films where the mass can be measured, but this is not the case for the LBL films because of effects from the substrate. On the other hand, the cast films are not as uniform as the LBL films, which is found to impair the quantitative analysis. Therefore a two-step procedure was adopted in this work. First, experiments were performed with cast $V_2O_5 \cdot 1.6H_2O$ xerogel films to determine the mass and estimate the percentage of electrochemically active sites. Then, the absorbance studies with the LBL films were carried out.

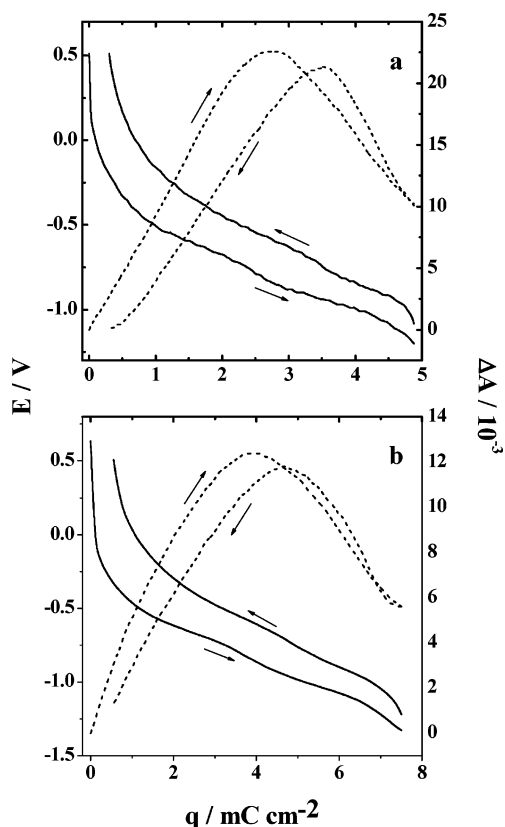


Figure 1. Chronopotentiometric curves (—) and absorbance change at 660 nm (---) for (a) 7.3 μg of cast V₂O₅·1.6H₂O xerogel and (b) 15-bilayer LBL films of V₂O₅/blend in 0.5 M LiClO₄/PC. $j = 10 \mu\text{A cm}^{-2}$.

The cast V₂O₅·1.6H₂O xerogel film had a mass measured with EQCM of 7.3 μg (3.46×10^{-8} mol). The chronopotentiometric curves and absorbance changes (ΔA) at 660 nm obtained with this cast film at a current density of $10 \mu\text{A cm}^{-2}$ are shown in Figure 1a. As a consequence of the electronic charge injection, lithium ions are intercalated/deintercalated into the V₂O₅ xerogel film during the reduction/oxidation processes. The wavelength of 660 nm was chosen to estimate the number of sites in the host matrix, because the V₂O₅ xerogel absorbance above 600 nm is attributed to the intervalence transfer V(IV) \rightarrow V(V).^{7,8} ΔA reaches a maximum value (ΔA_{max}) at ca. 2.7 mC cm^{-2} during the reduction process, where the number of V(IV) ions ($N_{\text{V(IV)}}$) is equal to that of V(V) ($N_{\text{V(V)}}$), considering only the electroactive sites. Upon a further increase in the charge injected, ΔA decreases due to an excess of V(IV) sites in comparison with V(V) (Figure 1a). Assuming that all the electrons injected just transform V(V) sites into V(IV) ones, these results suggest an amount of ca. 2.8×10^{-8} mol cm^{-2} (mol per centimeter square of geometric electrode area) of V₂O₅ sites participating in the redox process. This value corresponds to ca. 80% of the total sites under the experimental conditions used. The remaining 20% of the sites are electrochemically inactive, probably due to the lack of electrical contact among part of the V₂O₅ particles. Moreover, VO₄ sites are not involved in the conduction path because of the high potential barrier for electron hopping between 4-fold-coordinated ions. Thus electron hopping occurs preferentially between 5-fold coordinated vanadium ions.^{16,18} The number of electrochemically inactive V₂O₅ sites can also increase if access of lithium ions to some vanadium sites is hindered. Despite the small film thickness, approximately 30 nm estimated from the density of 1.5 g cm^{-3} for the xerogel,¹⁹ and of the low charge density applied ($10 \mu\text{A}$

cm^{-2}), diffusion effects could still interfere in the determination of the number of electroactive sites. These effects are likely to be small, and the conclusion about the presence of inactive V₂O₅ sites should be maintained. Indeed, Baddour et al. observed that 1.8 mol of electrons is injected for each mole of V₂O₅ xerogel under conditions that are close to equilibrium;²⁰ i.e., 90% of the sites are electroactive whereas the remainder 10% did not participate in the redox process. Significantly, from our results, the percentage of electroactive sites in the xerogel film, determined from the total injected charge and from the charge corresponding to the maximum absorbance change, is 75% and 80%, respectively. This agreement may be considered satisfactory, which validates the assumption made here that the absorbance change is correlated with the intervalence transfer V(IV) \rightarrow V(V), thus allowing the use of the quadratic logistic equation.

Figure 1b shows the chronopotentiometric curves at a current density of $10 \mu\text{A cm}^{-2}$ and ΔA values at 660 nm, for a 15-bilayer LBL film obtained from V₂O₅ xerogel nanocomposites by alternating V₂O₅ layers with the PEO–chitosan blend on ITO. Chitosan has indeed proven to be efficient in helping build the homogeneous LBL films, as only 1% of chitosan sufficed to obtain a good film from the blend.² Also, the electrochemical properties of V₂O₅ xerogel are preserved with the insertion of PEO. The chronopotentiometric curve of Figure 1b indicates an injected charge at ΔA_{max} of 3.94 mC cm^{-2} , corresponding to ca. 4.0×10^{-8} mol cm^{-2} of electrochemically active V₂O₅ sites. Considering that for each V₂O₅ electroactive site, two lithium ions can be injected,¹⁶ the maximum charge injected should be ca. 7.88 mC cm^{-2} , which is indeed close to the maximum charge obtained in the x-axis of Figure 1b (ca. 7.50 mC cm^{-2}). This suggests that the experimental conditions employed in this work allow an almost total reduction of the electroactive V₂O₅ sites.

A similar trend is observed for the absorbance changes as a function of charge when the potentiostatic method is employed, viz. cyclic voltammetry. The charge and ΔA values at 660 nm for 15-bilayer LBL films from V₂O₅/chitosan and V₂O₅/blend are shown in Figure 2a,b, respectively. An estimation of the number of electroactive V₂O₅ sites allows the separation of the contributions associated with transport effects (slow diffusion of lithium ions). ΔA_{max} occurs at 3.32 and 4.28 mC cm^{-2} for the two types of film, respectively. The V₂O₅/blend contains more electroactive sites (4.4×10^{-8} mol cm^{-2}) than V₂O₅/chitosan (3.4×10^{-8} mol cm^{-2}). The correlation between ΔA and the number of electrochemically active sites is supported by impedance data. Similarly to the ΔA values, the electronic conductivity in host matrixes is described in terms of the intervalence transfer V(IV) \rightarrow V(V).^{16,21} The bulk resistance (R_b) of the LBL films can be obtained from the log–log plot of the impedance modulus against frequency (Bode plot), shown in Figure 2c. R_b is ca. 1.5 and $7 \text{ k}\Omega \text{ cm}^2$ for V₂O₅/chitosan and 0.2 and $0.1 \text{ k}\Omega \text{ cm}^2$ for the V₂O₅/blend at -0.25 and -0.75 V , respectively. R_b depends on the potential because the conductivity varies with the oxidation state of the vanadium ions.²¹ The differences in conductivity for the two types of film are attributed to the amount of chitosan in the films, which favors electronic hindering and decreases the polaronic transfer flux V(IV) \rightarrow V(V) and the number of electroactive sites.

The ΔA data as a function of the charge injected can be explained quantitatively with the QLE (eq 2). Figure 3 shows the data of Figure 1b fitted with the QLE, for the reduction (Figure 3a) and oxidation (Figure 3b) processes. The values of r and K obtained from the fitting were $6 \text{ cm}^2 \text{ C}^{-1}$ and 8.0 mC

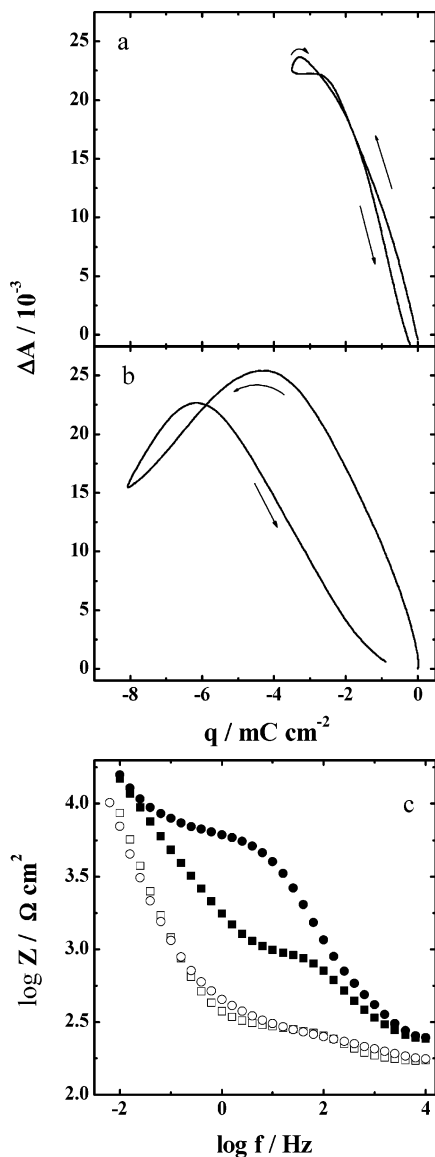


Figure 2. Plot of absorbance changes (at 660 nm) vs charge of cyclic voltammogram for 15-bilayer LBL films of (a) V_2O_5 /chitosan and (b) V_2O_5 /blend in 0.5 M $LiClO_4/PC$. $v = 20 \text{ mV s}^{-1}$. (c) Bode diagram for LBL films of V_2O_5 /chitosan (full) and V_2O_5 /blend (open) in 0.5 M $LiClO_4/PC$ at -0.25 V (square) and -0.75 V (circle) in 0.5 M $LiClO_4/PC$.

cm^{-2} , respectively, which means that the maximum charge injected is 8.0 mC cm^{-2} when all the $V(V)$ are reduced to $V(IV)$ and that $N_{V(V)} = N_{V(IV)}$ for 4 mC cm^{-2} .²² The theoretical plot departs from the experimental data when the charge injected is greater than 6.5 mC cm^{-2} (Figure 3a) and during deintercalation of the lithium ions (Figure 3b). A significant hysteresis is also observed between the reduction and oxidation processes. This hysteresis is also observed in the cyclic voltammograms and is attributed to structural changes in the xerogel, as discussed below.

The departure from the theoretical prediction is attributed to structural changes during the intercalation of lithium ions,²⁰ which are reflected in the absorbance spectrum.^{23,24} When the local or long-range order of the sample is decreased, the energy states can split, leading to states in the forbidden gap, which are originated by distortions of energy bands due to random fluctuations of the electric field.⁷ Figure 4 shows three absorbance spectra for values between 460 and 670 nm, at 0, 6, and 30 mC cm^{-2} for a 60-bilayer LBL film deposited on both sides

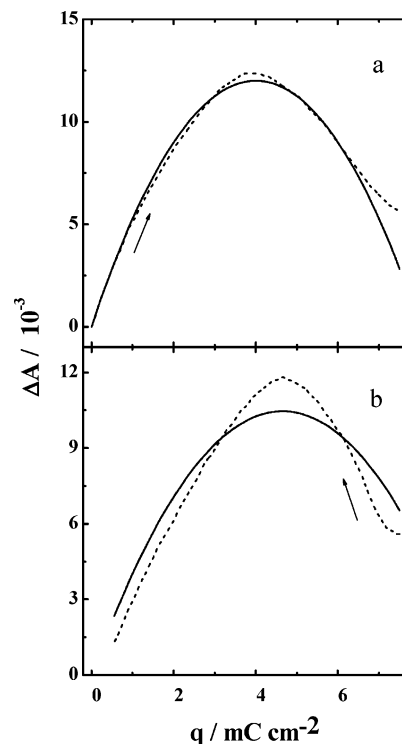


Figure 3. Plot of the (—) theoretical and (---) experimental ΔA data at 660 nm as a function of charge for 15-bilayer LBL films of V_2O_5 /blend (b) in 0.5 M $LiClO_4/PC$. $j = 10 \mu\text{A cm}^{-2}$.

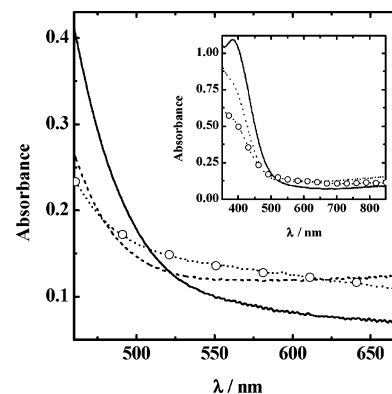


Figure 4. UV-visible spectra for 15-bilayer LBL films of V_2O_5 /blend at charge injected of (—) 0, (---) 6, and (· · ·) 30 mC cm^{-2} . The inset shows the absorbance spectra between 350 and 850 nm.

of the ITO substrate: a conducting side covered ITO and an insulating one formed by the bare glass. Thus, only the absorbance of the film adsorbed on the ITO side changes as a function of the charge injected. The inset in the figure shows the three absorbance spectra for a wider wavelength range (350–850 nm). The beginning of the absorbance edge depends on the charge injected, being extended to larger wavelengths for 30 mC cm^{-2} in comparison to the spectra for 0 and 6 mC cm^{-2} . This dependence is associated with the splitting of energy states in the forbidden gap due to structural changes. So, the overlapping of this absorbance change with that from the intervalence transfer ($> 600 \text{ nm}$) is responsible for the differences between theory and experiment for large amounts of intercalated lithium ions.

Structural changes are responsible for the slight potential change in Figure 1 at ca. -0.84 V during intercalation of lithium ions,²⁵ which promotes a greater accommodation of lithium ions in the V_2O_5 sites. The electrochemical profile changes associated with structural changes are better visualized in Figure 5, which

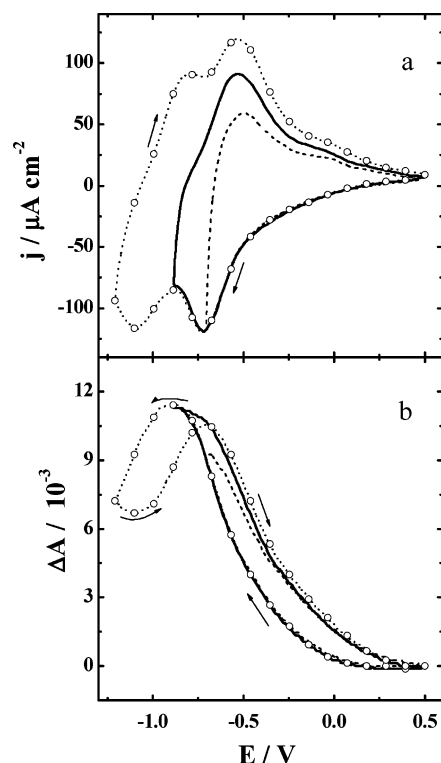


Figure 5. (a) Cyclic voltammetry and (b) absorbance plots for 8-bilayer LBL films of V₂O₅/blend between (---) +0.5 and −0.7 V, (—) +0.5 and −0.89 V, and (—○—) +0.5 and −1.2 V in 0.5 M LiClO₄/PC. $\nu = 20 \text{ mV s}^{-1}$.

shows the presence of the second voltammetric peak for a 8-bilayer LBL film of V₂O₅/blend. This voltammetric profile is similar to others reported in the literature.²⁶ Three potential ranges were used, viz. from +0.5 to −0.7 V, from +0.5 to −0.89 V and from +0.5 to −1.2 V (Figure 5a). The hysteresis in the ΔA curves increases significantly for $E < -0.89 \text{ V}$ because of the structural changes (Figure 5b). For example, coordination symmetry changes alter the polaron conduction pathway (and consequently the number of accessible sites) due to the potential energy change between vanadium atoms.¹⁸ It is also interesting to note that the beginning of the second voltammetric peak coincides with the maximum of ΔA during intercalation of lithium ions. Thus, on the basis of the absorbance changes due to intervalence transfer, the most significant structural changes occur when $N_{V(V)} = N_{V(IV)}$.

The fittings of the ΔA curves in Figure 5 using the QLE are shown in Figure 6. The resulting r and K values are $9.8 \pm 0.2 \text{ cm}^2 \text{ C}^{-1}$ and $4.55 \pm 0.05 \text{ mC cm}^{-2}$, respectively, during the ionic intercalation for all the potential ranges employed. For the ionic deintercalation process, r did not vary substantially in the three ranges ($r = 6.0 \pm 0.5 \text{ cm}^2 \text{ C}^{-1}$). However, the value of K obtained by fitting the absorbance in the potential range from +0.5 to −1.2 V (6.5 mC cm^{-2}) differs considerably from the value obtained from the fitting for the other potential ranges (14.0 mC cm^{-2}). Hence, significant differences between the theoretical and experimental data during the deintercalation of lithium ions are observed for $E < -0.89 \text{ V}$. This is in agreement with the hysteresis shown in Figure 5, attributed to structural changes.

In addition to a phenomenological understanding of the intervalence transfer, the QLE allows the determination of the number of electrochemically active sites, which can be correlated with the electrochemical profile. The QLE can also be used as a calibration curve for a quantitative determination of V(IV)

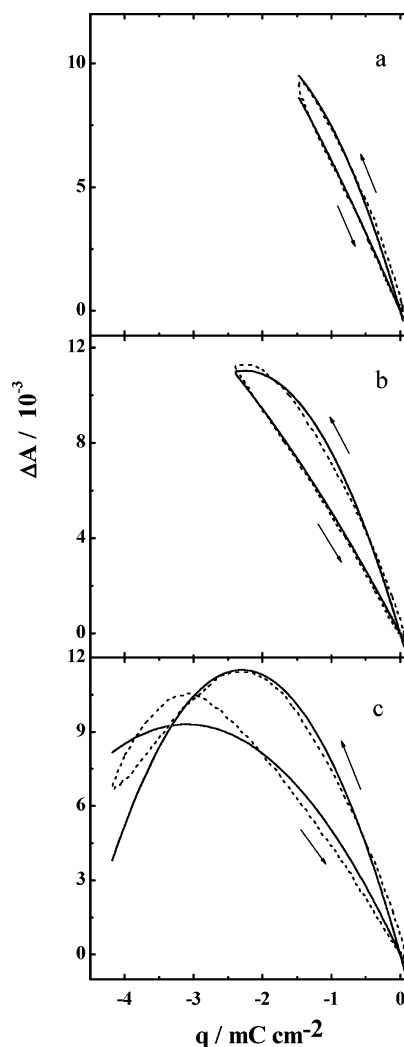


Figure 6. Plot of the (—) theoretical and (···) experimental ΔA data at 660 nm as a function of charge for 8-bilayer LBL films of V₂O₅/blend between (a) +0.5 and −0.7 V, (b) +0.5 and −0.89 V, and (c) +0.5 and −1.2 V in 0.5 M LiClO₄/PC. $\nu = 20 \text{ mV s}^{-1}$.

sites involved in chemical reactions. For example, it has been shown that V₂O₅ in nanocomposites formed from PEO suffers reduction when exposed to irradiation from a Hg lamp due to the photodegradation of PEO.²⁷ Based on theoretical ΔA curves shown above at 660 nm for a 15-bilayer LBL film from V₂O₅/blend ($\Delta A = 6q(1 - q/8)$), it is possible to determine $N_{V(IV)}$ ($=q/96500$) for the film exposed to a Hg lamp. For 1 and 4 h of exposure, the LBL film presented an absorbance of 0.114 and 0.147 at 660 nm, respectively. ΔA is 0.012 and 0.045, respectively, when the absorbance is compared to that of the nonirradiated film (0.102 at 660 nm). Using the QLE with $r = 6 \text{ cm}^2 \text{ C}^{-1}$ and $K = 8 \text{ mC cm}^{-2}$, it can be estimated that irradiation with a Hg lamp caused the formation of 2.07×10^{-8} and 7.78×10^{-8} mols of V(IV) for 1 and 4 h of exposure, respectively.

Conclusions

The absorbance changes associated with the V(IV) \rightarrow V(V) transition can be quantitatively analyzed with the quadratic logistic equation (QLE), allowing the determination of the number of electrochemically active sites. This defines the maximum charge that may possibly be injected into the V₂O₅ xerogel, regardless of the diffusion rate of lithium ions. The method to determine the number of V(IV) sites is extremely

important for LBL films, as it provides an estimate of the amount of V_2O_5 in the LBL film. On the other hand, the homogeneity of the LBL films allows the fitting of the experimental data for the intervalence transfer absorbance changes. Using the QLE, it is possible to analyze the polaron transfer as a function of the number of lithium ions intercalated into the nanostructured V_2O_5 xerogel matrix. From the parameters obtained from the fitting, it is also possible to determine the number of electroactive sites and the amount of V(IV) sites produced in chemical reactions. Moreover, the electrochemical profile can be better interpreted with the QLE, as indicated by the observation of structural distortions for $\Delta A = K/2 (N_{V(IV)} = N_{V(V)})$. Non-Faradaic processes and/or parallel reactions in materials containing V_2O_5 can be detected by this procedure and conductive pathways in such materials may be compared qualitatively.

Acknowledgment. Financial support from FAPESP, CNPq and Capes (Brazil) is gratefully acknowledged.

References and Notes

- (1) Ferreira, M.; Huguenin, F.; Zucolotto, V.; da Silva, J. E. P.; de Torresi, S. I. C.; Temperini, M. L. A.; Torresi, R. M.; Oliveira, O. N., Jr. *J. Phys. Chem. B* **2003**, *107*, 8351.
- (2) Huguenin, F.; dos Santos, D. S.; Bassi, A.; Nart, F. C.; Oliveira, O. N. *Adv. Funct. Mater.* **2004**, *14*, 985.
- (3) Oliveira, O. N.; He, J.-A.; Zucolotto, V.; Balasubramanian, S.; Li, L.; Nalwa, H. S.; Kumar, J.; Tripathy, S. K. In *Handbook of Polyelectrolytes and Their Applications*, 1st ed.; Tripathy, S. K., Kumar, J., Nalwa, H. S.; American Scientific Publishers: Los Angeles, 2002; Vol. 1, p 1.
- (4) Tarascon, J.-M.; Armand, M. *Nature* **2001**, *414*, 359.
- (5) Passerini, S.; Tipton, A. L.; Smyrl, W. H. *Sol. Energy Mater. Sol. Cells* **1995**, *39*, 167.
- (6) Austin, I. G.; Mott, N. F. *Adv. Phys.* **1969**, *18*, 41.
- (7) Bullo, J.; Cordier, P.; Gallais, O.; Gauthier, M.; Babonneau, F. *J. Non-Cryst. Solids* **1984**, *68*, 135.
- (8) Anaissi, F. J.; Demets, G. J. F.; Toma, H. E. *Electrochem. Commun.* **1999**, *1*, 332.
- (9) Croce, F.; Appetecchi, G. B.; Persi, L.; Scrosati, B. *Nature* **1998**, *394*, 456.
- (10) Guzmán, J.; Saucedo, I.; Navarro, R.; Revilla, J.; Guibal, E. *Langmuir* **2002**, *18*, 1567.
- (11) Strogatz, S. H. *Non Linear Dynamics and Chaos*; Addison-Wesley Publishing Co.: Reading, MA, 1994; p 353.
- (12) May, R. M. *Nature* **1976**, *261*, 459.
- (13) Gonzalez, E. R. *J. Electrochem. Soc.* **1996**, *143*, L113.
- (14) Torresi, R. M.; Cordoba de Torresi, S. I.; Gonzalez, E. R. *J. Electroanal. Chem.* **1999**, *461*, 161.
- (15) Bullo, J.; Gallais, O.; Gauthier, M.; Livage, J. *Appl. Phys. Lett.* **1980**, *36*, 986.
- (16) Livage, J. *Chem. Mater.* **1991**, *3*, 578.
- (17) dos Santos, D. S.; Bassi, A.; Rodrigues, J. J.; Misoguti, L.; Oliveira, O. N.; Mendonça, C. R. *Biomacromolecules* **2003**, *4*, 1502.
- (18) Nabavi, M.; Sanchez, C.; Livage, J. *Philos. Mag. B* **1991**, *63*, 941.
- (19) Liu, Y.-J.; Cowen, J. A.; Kaplan, T. A.; DeGroot, D. C.; Schindler, J.; Kannewurf, C. R.; Kanatzidis, M. G. *Chem. Mater.* **1995**, *7*, 1616.
- (20) Baddour, R.; Pereira-Ramos, J. P.; Messina, R.; Perichon, J. *J. Electroanal. Chem.* **1991**, *314*, 81.
- (21) Bullo, J.; Cordier, P.; Gallais, O.; Gauthier, M.; Livage, J. *J. Non-Cryst. Solids* **1984**, *68*, 123.
- (22) Varela, H.; Torresi, R. M.; Gonzalez, E. R. *Quim. Nova* **2002**, *25*, 99.
- (23) Huguenin, F.; Torresi, R. M.; Buttry, D. A. *J. Electrochem. Soc.* **2002**, *149*, A546.
- (24) Huguenin, F.; Torresi, R. M. *J. Braz. Chem. Soc.* **2003**, *14*, 536.
- (25) Pereira-Ramos, J.-P.; Baffier, N.; Pistoia, G. In *Lithium Batteries – New Materials, Developments and Perspectives*, 1st ed.; Pistoia, G., Ed.; Elsevier: Amsterdam, 1994; Vol. 1, p 281.
- (26) Wong, H. P.; Dave, B. C.; Leroux, F.; Harreld, J.; Dunn, B.; Nazar, L. F. *J. Mater. Chem.* **1998**, *8*, 1019.
- (27) Liu, Y.-J.; Schindler, J. L.; DeGroot, D. C.; Kannewurf, C. R.; Hirpo, W.; Kanatzidis, M. G. *Chem. Mater.* **1996**, *8*, 525.